Wider Channel Attention Network for Remote Sensing Image Super-resolution

Jun Gu, Guangluan Xu, Yue Zhang, Xian Sun, Ran Wen and Lei Wang.

***Abstract*—Recently, deep convolutional neural networks (CNNs) have obtained promising results in image processing tasks including super-resolution (SR). However, most CNN-based SR methods treat low-resolution (LR) inputs and features equally across channels, rarely notice the loss of information flow caused by the activation function and fail to leverage the representation ability of CNNs. In this letter, we propose a novel single-image super-resolution (SISR) algorithm named Wider Channel Attention Network (WCAN) for remote sensing images. Firstly, the channel attention mechanism is used to adaptively recalibrate the importance of each channel at the middle of the wider attention block (WAB). Secondly, we propose the Local Memory Connection (LMC) to enhance the information flow. Finally, the features within each WAB are fused to take advantage of the network's representation capability and further improve information and gradient flow. Analytic experiments on a public remote sensing data set (UC Merced) show that our WCAN achieves better accuracy and visual improvements against most state-of-the-art methods.**

***Index Terms*—remote sensing image, super-resolution, convolutional neural network, image fusion.**

I. Introduction

SINGLE image super-resolution (SISR) [1] aims to reconstruct a visually pleasing high-resolution (HR) image given its low-resolution (LR) input counterpart. The acquired HR images with detailed textures and critical information play an essential part in later remote sensing image analysis, such as target detection and object recognition. However, SISR is an ill-posed problem due to the loss of high-frequency information for LR images. Recently, many learning based methods have been proposed to tackle such an inverse problem.

In recent years, the methods based on deep convolutional neural networks (CNNs) have achieved significant improvements over conventional methods in the super-resolution task of remote sensing image processing field. Liebel et al. [2] firstly utilized a fully convolutional neural network named SRCNN [3] for multispectral satellite image super-resolution. Lei et al. [4] proposed an algorithm named local-global combined networks (LGCNet) to learn multilevel representations of remote sensing images. Kim et al. [5] achieved vast improvements over SRCNN by cascading small filters many times in a deep network structure (VDSR). Kim et al. [6] further proposed a deeply recursive convolutional network (DRCN) to reuse weight parameters while exploiting a large image context efficiently. Lim et al. [7] achieve a good result by redesigning the conventional residual networks and expanding the model size (EDSR). Yu et al. [8] recovered the low-resolution images by extending the features before activation function with the same parameters and yield the best result (WDSR). The above approaches have improved the indicators, but there remain three issues to be noticed.

First, most related works neglect the different importance among feature channels. However, the convolutional feature channels often attach different characteristics [9]. In the field of SISR, almost all of the methods above never utilize the channel attention mechanism to rescale each channel-wise feature adaptively. To the best of our knowledge, RCAN [10] first applied attention module to their work but only using the average strategy, which will weaken the salient features.

Second, WDSR has proved that the non-linear ReLUs will impede the information flow from shallow layers to deeper ones. The neural network in SISR now tends to go deeper, while the deeper network will contain more ReLU layers. Therefore, the obstruction of information flow will have a greater impact on deeper networks and affect the performance of this task, so this problem should be further addressed.

Third, the related SR studies do not under-use the representation ability of network. For deep neural networks in super-resolution tasks, the high utilization of features is one key to improve network representation capability and the final performance. However, for most existing work, they only use cross-block features without fully exploiting these features inside each block.

To solve these problems, we propose a novel residual block named wider attention block (WAB) in our network. The entire network is mainly composed of a stack of WABs, and our network has better reconstruction ability and high feature utilization. The contributions of this work are as follows:

(1) Attention Module: At the middle of each block, we use the channel attention module to recalibrate the channel significance of input features adaptively. Within this module, we take into account the overall effect and highlights by using both average and max strategies.

(2) Local Memory Connection: The Local Memory Connection (LMC) is proposed to enhance the information flow. Thus the features of the later layers can be compensated by the previous layers for better dense pixel value predictions.

(3) Feature Fusion: We extract the features inside each block and aggregate them simultaneously to make full use of the features and improve the flow of information and gradient.

J. Gu, G. Xu, Y. Zhang, R. Wen, X. Sun and L. Wang are with the Key Laboratory of Technology in Geo-spatial Information Processing and Application System, Institute of Electronics, Chinese Academy of Sciences, Beijing 100190, China (e-mail: dungu1995@163.com; wanglei@mail.ie.ac.cn).

J. Gu is with the School of Electronic, Electrical and Communication Engineering, University of Chinese Academy of Sciences, Beijing 100049, China.

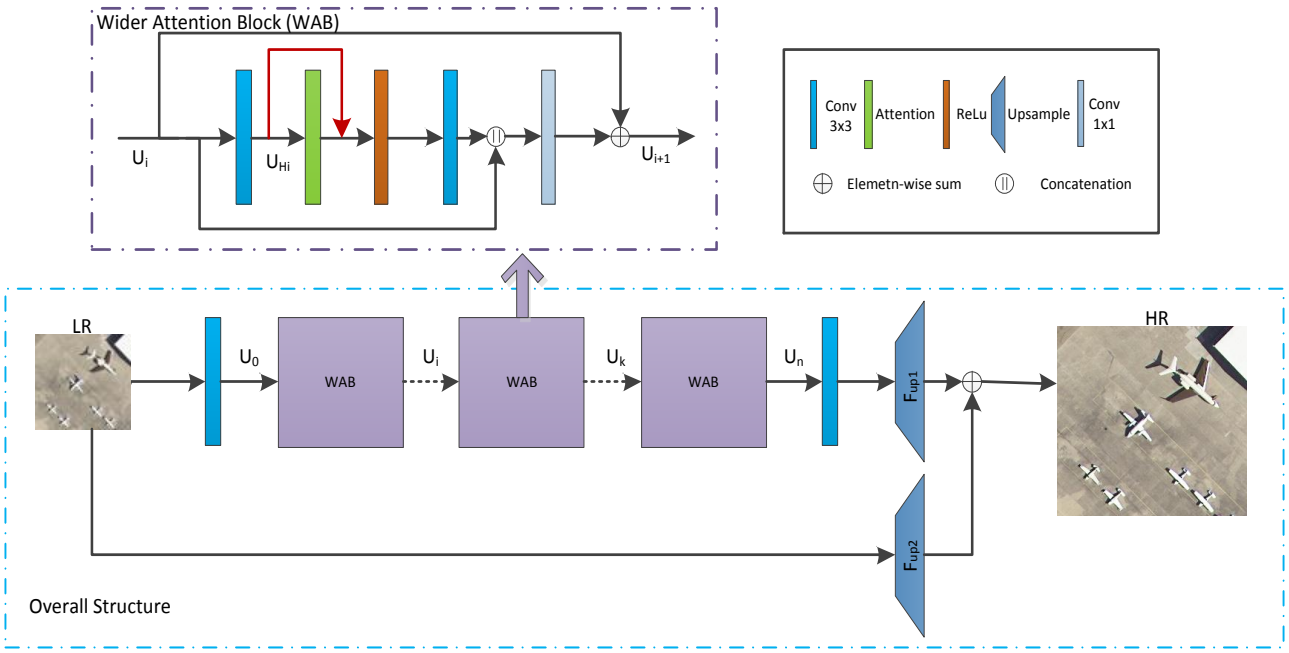

Fig. 1. Network architecture of our wider channel attention network (WCAN).

(4) Wider Attention Block: Based on the three strategies raised above, we propose the structure of WAB. In the task of SISR, the main body of the nerual network can be simply stacked by several WABs for better performance. We experimentally show that the modified sturcture of block produces better results.

II. Proposed Method

In this section, we will formulate the proposed method, including the Wider Attention Block and the overall structure.

A. Wider channel attention network (WCAN)

The overall structure of WCAN is illustrated in Fig. 1. Our WCAN can be decomposed into two branches: the identity branch and the residual branch. We take a low-resolution image as input X and learn an end-to-end mapping F from X to reconstructed HR image $\widehat{Y}$. On the residual branch, we use one convolution layer to extract features $\mathbf{U}_0$ directly from the LR input X. Then, several WABs are stacked to extract the features. Supposing there are N WABs, the output $\mathbf{U}_0$ and $\mathbf{U}_i$ can be obtained by:

$$\begin{aligned} \mathbf{U_0} &= \sigma(W_0 \cdot X + b_0) \\ \mathbf{U_i} &= \sigma(W_i \cdot U_{i-1} + b_i) \end{aligned} \tag{1}$$

where W_i, b_i, and σ represents the filters, bias, and the non-linear function respectively. The subscript $i \in (1, ..., N)$. The size of W_i is $c_i \times f_i \times f_i \times n_i$, where c_i is the number of input channels of the i_{th} convolutional layer, f_i is the spatial size of a filter, and n_i is the number of filters. b_i is of size n_i.

Then the output of the last wider attention block U_n will be fed into a convolutional layer. We adopt the sub-pixel module as the reconstruction part. About the identity branch, we use the same way to upsample the input image X. At last, we estimate the HR image via an element-wise summation, which can be formulated as:

$$\widehat{Y} = F_{up1}(F_{conv}(\mathbf{U_n})) + F_{up2}(X) \tag{2}$$

where F_{up1} and F_{up2} refer to the reconstruction layers on the residual branch and identity branch respectively. F_{conv} is the convolutional layer at the tail of main body.

B. Wider channel attention feature fusion block (WCAB)

Our wider channel attention block is built upon the channel attention, local memory connection and features fusion. The whole block is illustrated in Fig. 1. Let $\mathbf{U_i} \in R^{H \times W \times C}$ denotes the input of the $(i+1)_{th}$ WAB, where C represents the number of feature map channels.

Attention Module: A general and lightweight channle attention mechanism is introduced in the RCAN study, which allows for global information to selectively emphasize informative features and restrain less useful ones with a weight vector. Different from this module in RCAN, which only uses the global average pooling to take the channel-wise global spatial information into a descriptor, we aggregate these spatial information by using both average-pooling and max-pooling operations as illustrated in Fig. 2. The two different channel descriptors in our WAB can be formulated as:

$$\begin{aligned} \mathbf{U_i^{avg}} &= H_{GP}(\mathbf{U_i}) \\ \mathbf{U_i^{max}} &= H_{MP}(\mathbf{U_i}) \end{aligned} \tag{3}$$

where $H_{GP}(\cdot)$ and $H_{MP}(\cdot)$ are the global pooling and max pooling function.

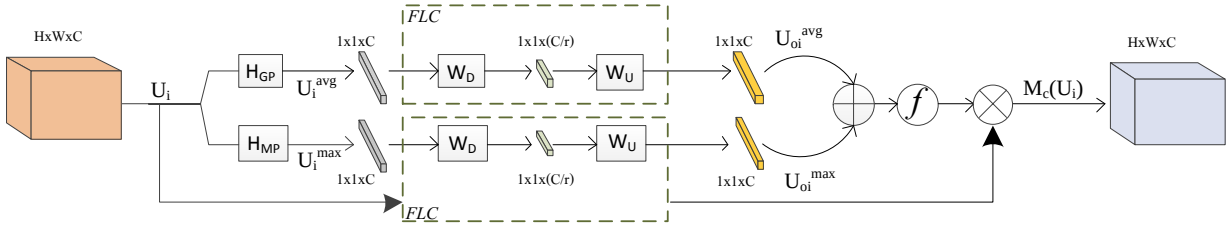

Fig. 2. Channel Attention (CA). $\otimes$, $\oplus$, and f denote elements-wise product, element-wise sum and activation function respectly.

TABLE I
BENCHMARK RESULTS. AVERAGE PSNR/SSIM FOR SCALE FACTOR $\times 2$, $\times 3$ AND $\times 4$. RED COLOR INDICATES THE BEST PERFORMANCE AND BLUE COLOR INDICATES THE SECOND BEST PERFORMANCE.

Dataset	Scale	Bicubic	SRCNN	VDSR	LGCNet	EDSR	WDSR	Ours
UCMerced	$\times 2$	31.081/0.8316	31.062/0.8428	33.804/0.8909	33.795/0.8817	34.748/0.9011	34.823/0.9102	34.883/0.9154
	$\times 3$	27.592/0.6557	28.241/0.6998	29.620/0.7350	29.637/0.7359	30.555/0.7643	30.601/0.7698	30.712/0.7712
	$\times 4$	25.723/0.5800	26.077/0.5439	27.265/0.5763	27.311/0.5850	28.097/0.6473	28.127/0.6514	28.261/0.6627

TABLE II
COMPARATIVE EXPERIMENTS OF OUR MODEL ON UC MERCED FOR $2\times$ SR. REPLACING OR REMOVING EACH COMPONENT WILL DEGRADE PERFORMANCE.

LMC	Attention Type	Feature Fusion	Activation	PSNR
$\surd$	$\times$	$\surd$	None	34.791
$\surd$	max	$\surd$	Sigmoid	33.836
$\surd$	avg	$\surd$	Sigmoid	33.840
$\surd$	max+avg	$\surd$	TanH	34.786
$\times$	max+avg	$\surd$	Sigmoid	34.802
$\times$	$\times$	$\surd$	None	34.711
$\surd$	max+avg	$\times$	Sigmoid	34.763
$\surd$	max+avg	$\surd$	Sigmoid	34.883

Then both channel-wise descriptors are followed by a shared network, which is implemented by fully connected layers (FCL) as shown in Fig. 2, to generate the weight vector:

$$\begin{aligned} \mathbf{U_{oi}^{avg}} &= \mathbf{W_U}(\mathbf{W_D}(\mathbf{U_i^{avg}})) \\ \mathbf{U_{oi}^{max}} &= \mathbf{W_U}(\mathbf{W_D}(\mathbf{U_i^{max}})) \\ FLC(\mathbf{U_i}) &= f(\mathbf{U_{oi}^{avg}} + \mathbf{U_{oi}^{max}}) \end{aligned} \tag{4}$$

where f denotes the sigmoid function. W_D is the weight set of a fully connect layer, which acts as channel-downscaling with reduction ratio r. The low-dimension signal is then increased with ratio r by a channel-upscaling layer, whose weight set is W_U.

The final output of the recalibration (denoted as M_c) is acquired by rescaling the input features $\mathbf{U_i}$. In short, the channel attention module is computed as:

$$M_c(\mathbf{U_i}) = FLC(\mathbf{U_i}) \otimes \mathbf{U_i} \tag{5}$$

where $\otimes$ denotes element-wise multiplication.

Local Memory Connetion: Inspired by the main innovation of WDSR, we propose the local memory connections, as shown in Fig. 1 (the red line), to enhance information transfer while maintaining a high degree of nonlinearity in deep neural networks. Thus low-level SR features from previousr layers may be more natural to propagate to the later layers for better dense pixel value predictions. The function of local memory connection F_{LMC} can be formulated as:

$$F_{LMC}(\mathbf{U_{Hi}}) = \mathbf{U_{Hi}} + F_{Atten}(\mathbf{U_{Hi}}) \tag{6}$$

where $\mathbf{U_{Hi}}$, F_{Atten} represents the input of the channel attention block and the attention module in each WAB. The network with local memory connections back-propagates gradients to former layers and improves the results.

Feature Fusion: To make full use of the representations capability of deep CNNs model and further improve the information and gradient flow, unlike most of the exsiting works, the features inside each block are fused rather than only using the features across blocks. Then, we utilize a 1×1 convolution layer $F_{1\times1}$ to compress this dimension to C. The whole feature fusion module F_f in the block can be formulated as :

$$F_f(\mathbf{U_i}) = F_{1\times1}([\mathbf{U_i}, F_l(\mathbf{U_i})]) \tag{7}$$

where F_l denotes the layers before the concatenation and the symbol $[\cdot]$ is the concatenation operation.

L_1 loss function, which has been demonstrated to be more powerful for SR [11], is used to train the proposed network. Given an input LR image X, we optimize parameters $\Theta = W_i, b_i$ by minimizing the loss function between the ground truth HR image Y and reconstructed image $\widehat{Y}$. The loss function of our network is :

$$L(\Theta) = ||\mathrm{Y} - \widehat{Y}|| \tag{8}$$

where $\mathbf{Y}$ is the target ground truth. The loss is averaged over the training set.

III. EXPERIMENTAL RESULTS AND ANALYSIS

A. Dataset

To evaluate our method, we choose the UC Merced [12] dataset, which is composed of 2100 land-use scene images

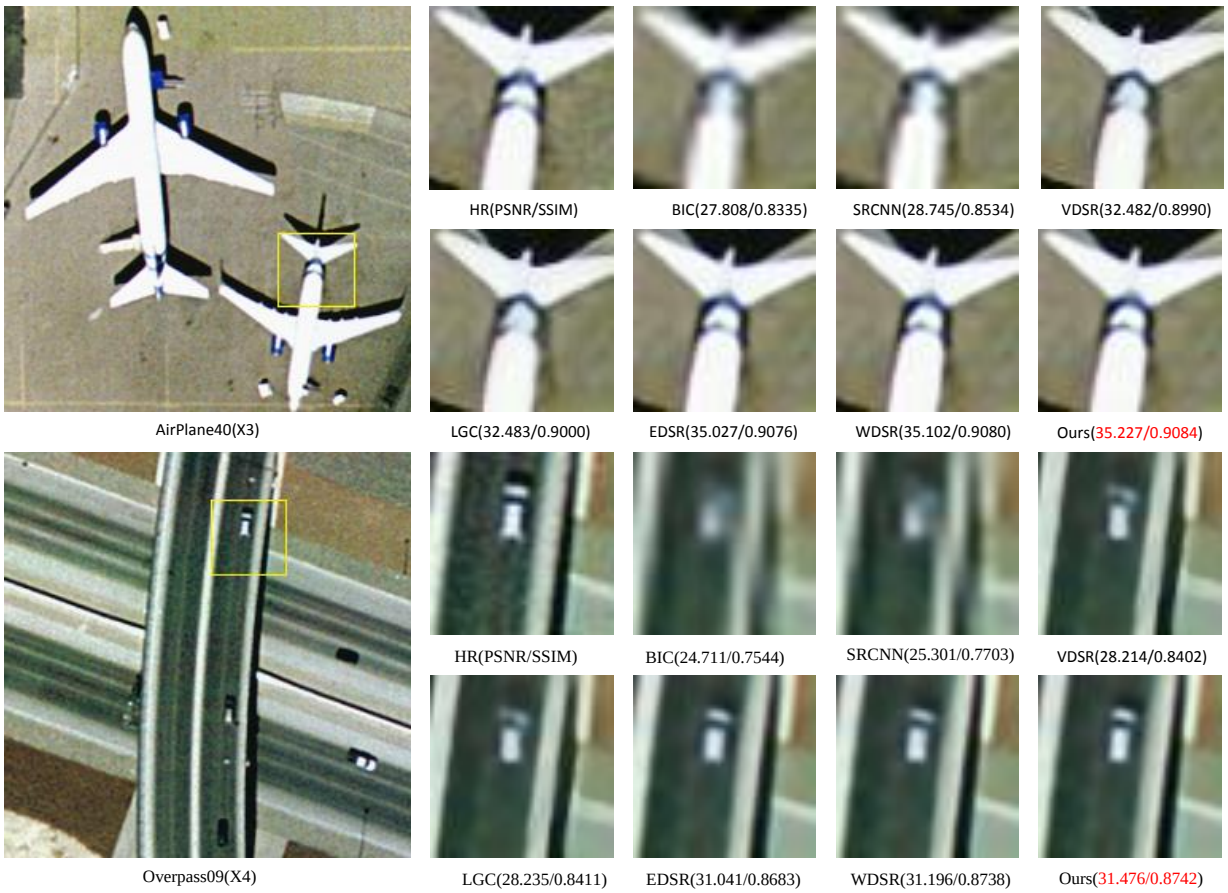

Fig. 3. Qualitative comparisons among these methods. In (a), the scale factor is $\times 3$, the stripe at the end of the plane is distinct. In (b), the edge of the car is more clearer with $\times 4$ scale factor. The Red color indicates the best performance.

measuring 256 256 pixels with relatively high spatial resolution (0.3 m/pixel). We randomly select 1700 images of the dataset for training and the others 400 of the samples as the testing set. Data augmentation is performed on the training images, which are randomly rotated by 90°, 180°, 270° and flipped horizontally. We downsample the original training images by scale factor 2, 3 and 4 and use the original images as high-resolution reference images.

B. Implementation Details

For training, we randomly crop 4848 image patches from the LR images as the input, and the corresponding HR image patches as the target.Our models are optimized with Adam [13] by setting $\beta 1 = 0.9$, $\beta 2 = 0.999$ and $\epsilon = 10^{-8}$. We set the initial learning rate to 1×10^{-3} and halve it decreased every 200 epochs. The batch size is set to 32. All convolutional filters (except the 1×1) have the same kernel size (3×3) and are initialized by the method of Xavier [14]. In this letter, we use the peak signal-to-noise ratio (PSNR) [dB] and structural similarity index measure (SSIM) [15] as criteria to evaluate the performance. We implement the proposed models via Pytorch framework and train them using NVIDIA Tesla P100 GPUs.

C. Results Comparison

We evaluate the performance of our proposed WCAN on the test set with different upsampling factors, compared with some other methods including bicubic interpolation, the classic CNN-based SRCNN, LGCNet, VDSR, EDSR and WDSR (state-of-the-art). For a fair and convincing comparison, we slightly adjust these methods and retrain these networks under our experimental dataset to obtain their best performance. Table I presents the ultimate mean PSNR and SSIM over the test images of these methods for three upsampling factors. Fig. 3 illustrates some super-resolution results of these methods compared with other methods, WCAN achieves the best performance with the highest PSNR and SSIM.

D. Wider Attention Block Analysis

The wider attention block is the most critical property in our network. To demonstrate the effect of each component in the block and verify the usefulness of this block, we carry out a set of experiments. For fairness, the number of features and blocks is changed to guarantee the same parameters. Table II shows the experiment results measured by the mean PSNR of the testing set, we can conclude from the result that the model with full components achieves the best performance.

TABLE III
MODEL COMPARISONS AT DIFFERENT PARAMETERS BUDGETS.

Residual Blocks	1	10	20
EDSR(PSNR/Para)	33.227/2.6M	34.052/26.2M	34.748/16.7M
WDSR(PSNR/Para)	33.301/0.8M	33.155/8.0M	34.823/14.8M
Ours(PSNR/Para)	33.356/0.8M	35.256/8.3M	34.883/15.7M

Attention Module. The attention module is the foundation of WAB. Therefore, we have done some researches on this module. Firstly, we run an ablation experiment to evaluate the effect of this module. Comparing the first and last columns of the results shown in Table II, the attention module can improve performance from 34.791dB to 34.883dB. This comparison firmly demonstrate the adaptive attentions to channel-wise features really improves the performance.

Secondly, within the attention module, average-pooling has been commonly adopted. However, the average-pooled features weakened the prominent part in one feature map. In that case, we use the max-pooling gathers another important clue about distinctive object features to infer the channel-wise attention. We verify that using both average-pooled and max-pooled features enables finer attention inference by comparing three variants of channel attention. The results in the second, third and the last columns can be proved that the max-pooled features can compensate the average-pooled features to infer a finer weight vector.

At last, we conjecture that the importance of feature maps will be further differentiated if using TanH which is distributed in both positive and negative domains. However, according to the result, this method is not in line with our expectations. Maybe TanH leads to more loss of useful information.

Local Memory Connection. The LMC is proposed in our network based on the importance of information flows for image super-resolution task. We carry out an ablation experiment of this skip connection. By removing this structure, our model falls back to a network similar to WDSR but with the channel attention in the middle of each block. In the fifth column, we remove the structure of LMC and the indicator has dropped a bit. The experiment confirms that LMC enhances the information flows and significantly improve the performance.

Feature Fusion. From the perspective of fully leveraging the representation capability of the network, the feature fusion component is proposed in our block. We designed a network without the feature fusion component for verification and find that the PSNR fall to 34.763dB. According to the results of last two columns, this component will significantly improve the performance. The possible reason is that the feature fusion will make full use of the features inside WAB and further enhance the information and gradient flow.

E. Model parameters and model depth

To compare the efficiency and accuracy at different model depth, a set of experiment is carried out for the task of image bicubic x2 super-resolution on our dataset. We mainly compare the number of parameters and validation PSNR to measure the two indicators above. Table III shows that our WCAN can achieve the most advanced performance when the number of parameters is similar to WDSR but less than EDSR. The model comparisons at different parameters budgets by controlling the number of blocks with a fixed number of channels.

IV. CONCLUSION

In this letter, we propose a novel network named WCAN for remote sensing image super-resolution. In WCAN, the proposed block uses a better approach to channel recalibration of input features and then the different level features are extracted and fused. In addition, the local memory connection in the residual branch and the upsampling module in the identity branch can reconstruct more details. Our network achieves a better result than WDSR by using the tricks above. Experimental results on the benchmark test dataset demonstrate that the proposed method can guarantee accurate results and outperform all existing state-of-the-art SR methods

REFERENCES

[1] D. Glasner, S. Bagon, and M. Irani, "Super-resolution from a single image," in *IEEE International Conference on Computer Vision*, 2009, pp. 349–356.

[2] L. Liebel and M. Körner, "Single-image super resolution for multispectral remote sensing data using convolutional neural networks." *International Archives of the Photogrammetry, Remote Sensing & Spatial Information Sciences*, vol. 41, 2016.

[3] C. Dong, C. L. Chen, K. He, and X. Tang, *Learning a Deep Convolutional Network for Image Super-Resolution*. Springer International Publishing, 2014.

[4] S. Lei, Z. Shi, and Z. Zou, "Super-resolution for remote sensing images via local-global combined network," *IEEE Geoscience & Remote Sensing Letters*, vol. PP, no. 99, pp. 1–5, 2017.

[5] J. Kim, J. K. Lee, and K. M. Lee, "Accurate image super-resolution using very deep convolutional networks," in *IEEE Conference on Computer Vision and Pattern Recognition*, 2016, pp. 1646–1654.

[6] J. Kim, J. Kwon Lee, and K. Mu Lee, "Deeply-recursive convolutional network for image super-resolution," in *Proceedings of the IEEE conference on computer vision and pattern recognition*, 2016, pp. 1637–1645.

[7] B. Lim, S. Son, H. Kim, S. Nah, K. M. Lee, B. Lim, S. Son, H. Kim, S. Nah, and K. M. Lee, "Enhanced deep residual networks for single image super-resolution," in *Computer Vision and Pattern Recognition Workshops*, 2017, pp. 1132–1140.

[8] J. Yu, Y. Fan, J. Yang, N. Xu, Z. Wang, X. Wang, and T. Huang, "Wide activation for efficient and accurate image super-resolution," *arXiv preprint arXiv:1808.08718*, 2018.

[9] Q. Wang, Z. Teng, J. Xing, J. Gao, W. Hu, and S. Maybank, "Learning attentions: residual attentional siamese network for high performance online visual tracking," in *Proceedings of the IEEE Conference on Computer Vision and Pattern Recognition*, 2018, pp. 4854–4863.

[10] Y. Zhang, K. Li, K. Li, L. Wang, B. Zhong, and Y. Fu, "Image super-resolution using very deep residual channel attention networks," 2018.

[11] H. Zhao, O. Gallo, I. Frosio, and J. Kautz, "Loss functions for image restoration with neural networks," *IEEE Transactions on Computational Imaging*, vol. 3, no. 1, pp. 47–57, 2017.

[12] Y. Yang and S. Newsam, "Bag-of-visual-words and spatial extensions for land-use classification," in *Sigspatial International Conference on Advances in Geographic Information Systems*, 2010, pp. 270–279.

[13] D. P. Kingma and J. Ba, "Adam: A method for stochastic optimization," *arXiv preprint arXiv:1412.6980*, 2014.

[14] X. Glorot and Y. Bengio, "Understanding the difficulty of training deep feedforward neural networks," in *Proceedings of the thirteenth international conference on artificial intelligence and statistics*, 2010, pp. 249–256.

[15] Z. Wang, A. C. Bovik, H. R. Sheikh, and E. P. Simoncelli, "Image quality assessment: from error visibility to structural similarity," *IEEE Trans Image Process*, vol. 13, no. 4, pp. 600–612, 2004.